2015

Modelling the shear behaviour of sedimentary rock joints under constant normal stiffness conditions

S Thirukumaran
University of Wollongong, ts377@uowmail.edu.au

B Indraratna
University of Wollongong, indra@uow.edu.au

E T. Brown
Golder Associates Pty Ltd

Publication Details

Thirukumaran, S., Indraratna, B. & Brown, E. T. (2015). Modelling the shear behaviour of sedimentary rock joints under constant normal stiffness conditions. 49th US Rock Mechanics / Geomechanics Symposium 2015 (pp. 2918-2922). United States: American Rock Mechanics Association.

Modelling the shear behaviour of sedimentary rock joints under constant normal stiffness conditions

Abstract

The typical shear behaviour of rock joints has been studied under a constant normal load (CNL) or zero normal stiffness condition, but recent studies have shown that this boundary condition may not replicate more practical situations, and that constant normal stiffness (CNS) is a more appropriate boundary condition to describe the stress-strain response of field joints. In addition to the effect of boundary conditions, the shear behaviour of a rough joint also depends on its surface properties and the initial stress acting on its interface. Despite this, exactly how these parameters affect the shear behaviour of joints is not fully understood because the stress-strain response of joints is governed by non-uniform asperity damage and the resulting gouge that accumulates on their interfaces. Therefore, an attempt has been made in this study to predict the complete shear behaviour of rough joints incorporating the asperity deformation under CNS conditions. In order to validate this analytical model, a series of CNS shear tests were conducted on rough tensile (natural) joints and their replicas at a range of initial normal stresses that varied from 0.4 to 1.6 MPa. Comparisons between the predicted shear behaviour and the experimental results show close agreement.

Disciplines

Engineering | Science and Technology Studies

Publication Details

Thirukumaran, S., Indraratna, B. & Brown, E. T. (2015). Modelling the shear behaviour of sedimentary rock joints under constant normal stiffness conditions. 49th US Rock Mechanics / Geomechanics Symposium 2015 (pp. 2918-2922). United States: American Rock Mechanics Association.

ARMA 15-232

Modelling the shear behaviour of sedimentary rock joints under constant normal stiffness conditions

Thirukumaran, S.
University of Wollongong, Wollongong, NSW, Australia
Indraratna, B.
University of Wollongong, Wollongong, NSW, Australia
Brown, E.T.
Golder Associates Pty Ltd, Brisbane, QLD, Australia

This paper was prepared for presentation at the 49th US Rock Mechanics / Geomechanics Symposium held in San Francisco, CA, USA, 28 June- 1 July 2015.

ABSTRACT: The typical shear behaviour of rock joints has been studied under a constant normal load (CNL) or zero normal stiffness condition, but recent studies have shown that this boundary condition may not replicate more practical situations, and that constant normal stiffness (CNS) is a more appropriate boundary condition to describe the stress-strain response of field joints. In addition to the effect of boundary conditions, the shear behaviour of a rough joint also depends on its surface properties and the initial stress acting on its interface. Despite this, exactly how these parameters affect the shear behaviour of joints is not fully understood because the stress-strain response of joints is governed by non-uniform asperity damage and the resulting gouge that accumulates on their interfaces. Therefore, an attempt has been made in this study to predict the complete shear behaviour of rough joints incorporating the asperity deformation under CNS conditions. In order to validate this analytical model, a series of CNS shear tests were conducted on rough tensile (natural) joints and their replicas at a range of initial normal stresses that varied from 0.4 to 1.6 MPa. Comparisons between the predicted shear behaviour and the experimental results show close agreement.

1. INTRODUCTION

An appropriate evaluation of the shear behaviour of rock joints is vital, for instance when analysing the stability of rock slopes, designing excavations in jointed rock, assessing the stability of concrete dam foundations, and designing rock socked piles. In conventional studies, the shear behaviour of a joint is usually investigated in the laboratory under constant normal load (CNL) boundary conditions where the normal stress remains constant and the surface of the joint dilates freely during shearing. However in engineering practice, the normal stress acting on the joint interface may vary during shearing, and the joint dilation may be constrained by the confined environment formed across the interface. This often represents a constant normal stiffness (CNS) condition. The practical implications of this are movements of unstable blocks in the roof or walls of an underground excavation, reinforced rock wedges sliding in a rock slope or foundation, and the vertical movement of rock-socketed concrete piles. Several researchers have emphasised the fact that a constant normal stiffness (CNS) boundary condition is more appropriate for many field situations [1-7].

To date, only a few methods have been proposed to model the shear behaviour of rough rock joints under CNS conditions [1, 5, 6, 8], but according to Indraratna and Haque [6], most of them do not allow for the complex joint surface characteristics and degradation behaviour of asperities under CNS conditions. It is therefore a key objective of this study to develop a simpler and more efficient analytical model that can represent the shear responses of natural rough rock joints and also capture the asperity damage occurring under the CNS stress history

2. DEVELOPMENT OF A NEW ANALYTICAL MODEL

2.1. Modelling of dilation behaviour of a joint

Fig. 1 shows the proposed conceptual variation of the dilation rate ($\dot{v}$) with the ratio of shear displacement to peak shear displacement (δ_h/δ_{h-peak}) for a joint subjected to direct shear under CNS; this variation in the rate of dilation can be characterised by three major zones on the basis of δ_h/δ_{h-peak}. As shearing begins, the contact asperities on the opposing joint surfaces will tend to compress elastically under the initial normal load and increased shear load, before sliding against each other [9]. This means that as shearing begins dilation will be postponed in a small range of shear displacement, so in the region defined by $c_0 < \delta_h/\delta_{h-peak} \le 1$, where the opposing asperities slide against each other along their point of contact, the rate of dilation rises to its peak value where $\delta_h/\delta_{h-peak} = 1$. Beyond the peak shear displacement (i.e. $\delta_h/\delta_{h-peak} > 1$), the dilation rate decreases continuously with shear displacement as the asperities at the joint interface are damaged [10]. To describe this variation in the rate of dilation for these three different zones, the following equations are proposed:

$$\dot{v} = \begin{cases} 0 & for \quad 0 < \left(\delta_h/\delta_{h-peak}\right) \le c_0 \\ \dot{v}_{peak}\left(1 - \dfrac{1}{(1-c_0)^2}\left(\dfrac{\delta_h}{\delta_{h-peak}} - 1\right)^2\right) & for \quad c_0 < \left(\delta_h/\delta_{h-peak}\right) \le 1 \\ \dot{v}_{peak}\exp\left(-\left(c_1\left(\dfrac{\delta_h}{\delta_{h-peak}} - 1\right)\right)^{c_2}\right) & for \quad \left(\delta_h/\delta_{h-peak}\right) > 1 \end{cases} \qquad (1a)$$

where, $\dot{v}$ = dilation rate, δ_h = shear displacement, δ_{h-peak} = shear displacement at peak stress ratio, c_0 = ratio of δ_h/δ_{h-peak} at which dilation is assumed to begin, c_1 and c_2 = decay constants and $\dot{v}_{peak}$ = peak dilation rate which can be calculated by following equation [11]:

$$\dot{v}_{peak} = \left(\frac{\tan\beta}{1 - \left(K_n\left(-\alpha \sec^2\beta + \lambda\right)\right)}\right) \qquad (1b)$$

in which,

$$\alpha = \left(\frac{\delta_{h-peak} \times JRC \times \pi}{M \times \ln 10 \times \sigma_{n0} \times 180}\right) \qquad (1c)$$

$$\beta = \frac{1}{M} \times JRC \times \log_{10}\left(\frac{JCS}{\sigma_{n0}}\right) \qquad (1d)$$

$$\lambda = \frac{k_{ni} \times V_m^{\ 2}}{\left(k_{ni} \times V_m + \sigma_{n0}\right)^2} \qquad (1e)$$

where K_n = external constant normal boundary stiffness, JRC = joint roughness coefficient, JCS = compressive strength of joint surface, M = damage coefficient which was either 1 or 2 for shearing under low normal stress or high normal stress, respectively, σ_{n0} = initial normal stress, k_{ni} = initial joint normal stiffness at zero normal stress and V_m = maximum closure of joint.

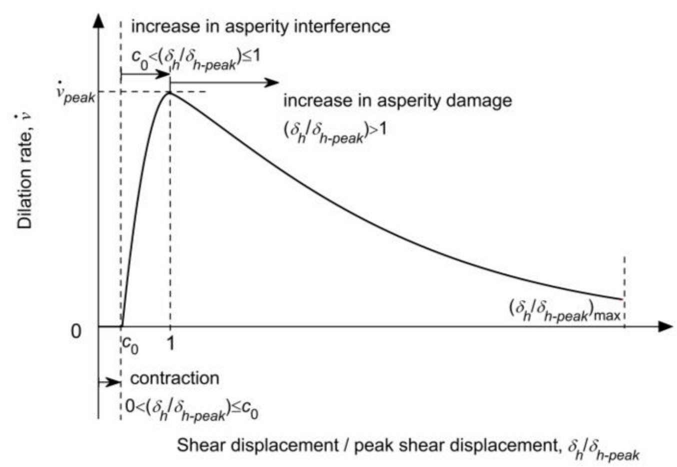

Fig. 1. Proposed concept to model the variation of dilation rate with shear displacement (after [11]).

2.2. Modelling the shear behaviour of a joint

When the variation in the dilation rate and the shear displacement are known, the dilation or normal displacement of joint δ_v for any shear displacement δ_h can be calculated as:

$$\delta_v = \int_0^{\delta_h} (\dot{v})\, d\delta_h \qquad (2)$$

In Eq. (2), $\dot{v}$ can be obtained from Eq. (1).

Under CNS conditions, the normal stress changes linearly with normal displacement, so the normal stress σ_n at any shear displacement δ_h can be expressed as:

$$\sigma_n = \sigma_{n0} + K_n \times \delta_v \qquad (3)$$

where σ_{n0} = initial normal stress and δ_v = normal displacement which can be calculated from Eq. (2).

By adopting the concept of mobilised roughness as proposed by Barton [12], the mobilised shear stress τ_{mob} for CNS condition can be expressed as:

$$\tau_{mob} = \sigma_n \times \tan\phi_{mob} \qquad (4)$$

in which, σ_n = normal stress at a shear displacement δ_h and can be calculated from Eq. (3), and ϕ_{mob} = mobilised friction angle that can be expressed as a summation of the basic friction angle ϕ_b and the dilation angle $i\ (= \arctan \dot{v})$, thus:

$$\phi_{mob} = \phi_b + i \qquad (5)$$

By combining Eqs. (2)-(5), the mobilised shear stress τ_{mob} for any shear displacement δ_h under CNS can be calculated by the following equation:

$$\tau_{mob} = \left(\sigma_{n0} + K_n \times \int_0^{\delta_h} (\dot{v}) d\delta_h \right) \left(\frac{\tan \phi_b + \dot{v}}{1 - \dot{v} \times \tan \phi_b} \right) \quad (6)$$

Eq. (6) can only be used to predict the shear behaviour of a joint when the asperities begin to mobilise at the joint interface, so Eq. (6) does not describe the shear behaviour within a small range of strain when shearing begins. By assuming the shear behaviour is elastic for the initial small range of shear displacement, the current shear stress τ for any shear displacement δ_h is given by:

$$\tau = \begin{cases} k_s \times \delta_h & if \quad k_s \times \delta_h < \tau_{mob} \\ \tau_{mob} & otherwise \end{cases} \quad (7)$$

where k_s = joint shear stiffness.

3. EXPERIMENTAL PROGRAM

3.1. Specimen preparation

Thirukumaran [13] has described the procedures for preparing rock joint specimens in detail, so only a summary will be given here. Three different types of sandstone blocks were split to expose the surfaces of natural rough joints. These surfaces were replicated with silicone rubber moulds which were then used to make replicas with high strength plaster (a sedimentary rock-like material) mixed with water at a ratio of 7:2 by weight. The upper and lower specimens were 120 mm long, 120 mm wide and 100 mm high. To achieve the desired strength before testing, all the specimens were cured for 2 weeks at a controlled temperature of 40 °C. The mean mechanical properties of this modelling material are shown in Table 1. These replicas of rough joints were called RSW, RSR and RSY, respectively.

Table 1. Mechanical properties of modelling material: uniaxial compressive strength (C_0), uniaxial tensile strength (T_0), basic friction angle (ϕ_b) and Young's modulus (E).

C_0	T_0	ϕ_b	E
65.6 MPa	6.3 MPa	30 deg	19.3 GPa

3.2. Characterisation of joint surface roughness

The joint surfaces were digitised with a 3D-laser scanner (Minolta vivid 910) having an accuracy of 100 µm and a precision of 8 µm. The digitised upper surface of the RSR joint is shown in Fig. 2, as an example. In order to quantify the roughness of the joint profiles, the most widely used correlation between the statistical roughness parameter Z_2 and JRC proposed by Tse and Cruden [14] was used in this study:

$$JRC = 32.2 + 32.47 \log Z_2 \quad (8)$$

where, JRC = joint roughness coefficient, and Z_2 = root mean square of the first derivative of the profile and can be expressed as:

$$Z_2 = \left(\frac{1}{L_n} \sum_{i=1}^{N_p - 1} \frac{(z_{i+1} - z_i)^2}{(x_{i+1} - x_i)} \right)^{1/2} \quad (9)$$

where, (x_i, z_i) and (x_{i+1}, z_{i+1}) = adjacent digitised coordinates of the profile separated by the sampling interval of Δx, N_p = number of digitised points and L_n = length of the joint profile. Eleven profiles that were parallel to shear direction (i.e. along the x direction) were selected from each digitised surface and placed 10 mm apart along the y direction.

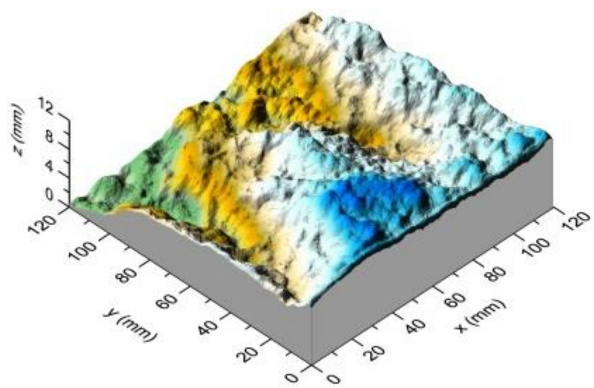

Fig.2. 3D digitised surface of RSR joint.

For each digitised joint profile on the joint surface, the JRC was calculated from Eq. (8) based on a sampling interval of 0.5 mm. The mean values of JRC were 7.3, 10.4 and 15.3 for the RSW, RSR and RSY joints; these respective values were then used to describe the roughness of each joint surface before shearing.

3.3. Testing procedure

An upgraded CNS direct shear apparatus with a servo-hydraulic controller was used in this study (see [11, 13]). The shear loads were applied with hydraulic jacks equipped with a servo unit, whereas the initial normal load was applied through a set of four springs with an overall stiffness of K_n = 0.8 kN/mm (= 0.56 MPa/mm for a joint area of 120×120 mm^2). The normal and shear displacements were measured through two LDVTs, and the normal and shear loads were measured through load cells with capacities of 180 and 120 kN, respectively. The tests were performed under initial applied normal stresses, σ_{n0} of 0.4, 0.8 and 1.6 MPa. A fresh specimen was sheared up to 15 mm at a constant shearing rate of 0.5 mm/min at each initial normal stress, and each shear test was repeated twice to ensure that the measured data was reliable.

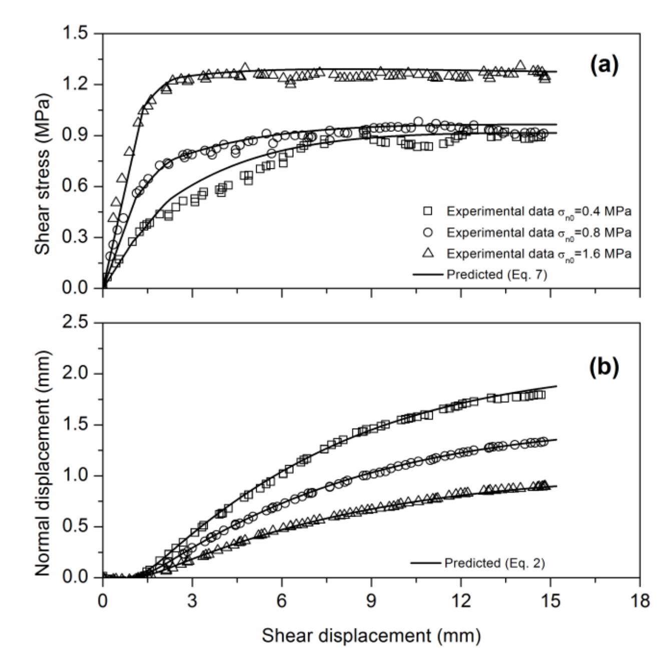

Fig. 3. Shear behaviour of joints with different levels of σ_{n0} under CNS for RSR joint (JRC = 10.4).

4. RESULTS AND DISCUSSION

4.1. Shear behaviour of joints

A set of CNS direct shear test results for the RSR (JRC =10.4) under three different initial normal stresses is shown in Fig. 3. It can be seen that for a small shear displacement (e.g., $\delta_h \approx$ 1-2 mm), the shear stress increased almost linearly with shear displacement (i.e., quasi-elastic phase), and then exhibited a slight strain-hardening behaviour (Fig. 3a). These shear stress-shear displacement plots do not indicate a distinct peak. This was caused by the increase in normal stress with shear displacement due to the external boundary stiffness. When the initial normal stress increased, the shear stress-displacement followed a ductile trend over a wide range of shear movement (3 mm $< \delta_h <$ 15 mm). This can be attributed to the compaction of gouge (following asperity damage) on both joint surfaces that negated the effect of the remaining asperities (i.e., reflecting the behaviour of a planar joint).

The normal displacement behaviour (volume change) showed an initially small contraction until a shear displacement of about 1 mm, followed by dilation and then a subsequent decrease in dilation with increasing initial normal stress σ_{n0} (Fig. 3b).

The effect of joint roughness on the shear behaviour of joints is shown in Fig. 4. As expected, the RSY joint (JRC =15.3) showed a higher value of shear stress than the RSR joint (JRC =10.4) and the RSW joint (JRC =7.3) under similar levels of initial normal stress (Fig. 4a). Fig. 4b confirmed that the joint with a higher roughness dilated more.

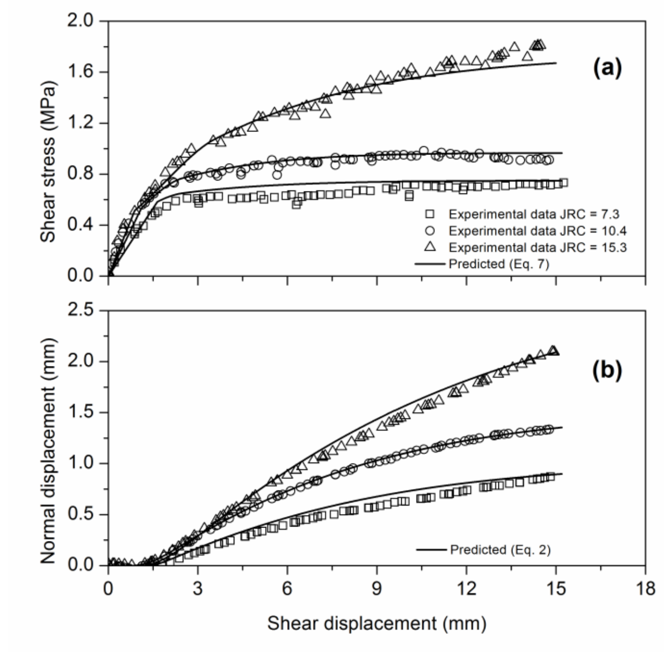

Fig. 4. Shear behaviour of joints with different JRC values under CNS at σ_{n0} = 0.8 MPa.

4.2. Comparison between predicted and experimental results

Through a non-linear regression analysis, the decay constants c_1 and c_2 for all three joints were found to be 0.3 and 1.2, respectively. Similarly, the value of c_0 was found to be around 0.3. The quantification of JRC was explained in the previous section. The JCS can be assumed to be C_0 because the joint surfaces were fresh. The joint normal deformational parameters V_m and k_{ni} were determined from joint closure tests (Table 2).

Table 2, Input parameters used for model prediction.

Joint type	σ_{n0} (MPa)	δ_{h-peak} (mm)	$(-)^a k_{ni}$ (MPa/mm)	$(-)^a V_m$ (mm)	k_s (MPa/mm)
RSW	0.8	2.35	5.35	0.43	0.36
RSR	0.4	2.3	9.83	0.44	0.27
	0.8	2.4			0.48
	1.6	2.5			0.78
RSY	0.8	3.45	10.1	0.34	0.58

[a] negative sign used as sign convention

Figs. 3 and 4 show that the predicted values of shear stress (Eq. (7)) and dilation (Eq. (2)) agreed with the experimental results for the RSW, RSR and RSY joints. These validations confirmed that the proposed modelling approach described the real behaviour of rough joints under CNS once the characteristics of the joint surface were determined accurately.

5. CONCLUSIONS

An analytical model to predict the real shear behaviour of rock joints under CNS conditions has been proposed and validated with the experimental data. This approach demonstrated that by modelling the dilation behaviour of a joint under CNS, the complete shear behaviour of the joint under the CNS stress path can be described. The experimental results showed that the shear response of rough joints was greatly affected by damage to the asperities, the extent of which increased as the initial normal stress increased. Eq. (1) can capture the asperity damage under CNS along with other governing parameters such as joint surface roughness (JRC), the strength of the joint surface (JCS), and the initial applied normal stress (σ_{n0}) and boundary normal stiffness (K_n), but the model requires further validation to ensure that its predictions are accurate.

ACKNOWLEDGMENTS

The Authors would like to thank the Australian Research Council (ARC) Linkage Project for financial support. The Authors would also like to acknowledge Springer Publications for allowing us to use the technical data presented in numerous Figures and Tables, and some technical discussions in the paper published in the journal, Rock Mechanics and Rock Engineering Journal.

REFERENCES

[1] Heuze F. E. 1979. Dilatant effects of rock joints. Proc 4th ISRM Congress. Montreux. p. 169-75.

[2] Leichnitz W. 1985. Mechanical properties of rock joints. Int J Rock Mech Min Sci Geomech Abstr. 22(5):313-21.

[3] Johnston I. W., Lam T. S. K., and Williams A. F. 1987. Constant normal stiffness direct shear testing for socketed pile design in weak rock. Géotechnique. 37(1):83-9.

[4] Ohnishi Y., and Dharmaratne P. G. R. 1990. Shear behaviour of physical models of rock joints under constant normal stiffness conditions. In: Barton N, and Stephansson O, editors. Proc Int Conf on Rock Joints. Loen: Balkema. p. 267-73.

[5] Saeb S., and Amadei B. 1992. Modelling rock joints under shear and normal loading. Int J Rock Mech Min Sci Geomech Abstr. 29(3):267-78.

[6] Indraratna B., and Haque A. 2000. Shear Behaviour of Rock Joints. Rotterdam: Balkema.

[7] Jiang Y., Xiao J., Tanabashi Y., and Mizokami T. 2004. Development of an automated servo-controlled direct shear apparatus applying a constant normal stiffness condition. Int J Rock Mech Min Sci. 41(2):275-86.

[8] Skinas C. A., Bandis S. C., and Demiris C. A. 1990. Experimental investigations and modelling of rock joint behaviour under constant stiffness. In: Barton N, and Stephansson O, editors. Proc Int Conf on Rock Joints. Loen: Balkema. p. 301-8.

[9] Haberfield C. M., and Johnston I. W. 1994. A mechanistically-based model for rough rock joints. Int J Rock Mech Min Sci Geomech Abstr. 31(4):279-92.

[10] Plesha M. E. 1987. Constitutive models for rock discontinuities with dilatancy and surface degradation. Int J Numer Anal Meth Geomech. 11(4):345-62.

[11] Indraratna B., Thirukumaran S., Brown E. T., and Zhu S.-P. 2015. Modelling the shear behaviour of rock joints with asperity damage under constant normal stiffness. Rock Mech Rock Eng. 48(1):179-95.

[12] Barton N. 1982. Modelling rock joint behavior from in situ block tests: implications for nuclear waste repository design. Office of Nuclear Waste Isolation Report, Columbus, OH, ONWI-308.

[13] Thirukumaran S. 2014. Shear strength of degradable rock joints [PhD Thesis]. Australia: University of Wollongong.

[14] Tse R., and Cruden D. M. 1979. Estimating joint roughness coefficients. Int J Rock Mech Min Sci Geomech Abstr. 16(5):303-7.